Substorm triggering by poleward boundary intensification and related equatorward propagation

S. B. Mende,[1] H. U. Frey,[1] V. Angelopoulos,[2] and Y. Nishimura[3]

Received 31 May 2010; revised 17 November 2010; accepted 4 January 2011; published 5 April 2011.

[1] Recently, a revised auroral substorm onset sequence has been proposed, in which onset is preceded by a poleward boundary intensification (PBI) and subsequent equatorward propagation of N-S-aligned auroral features to breakup arc latitudes. We reanalyzed 20 randomly selected samples of the Nishimura et al. (2010) 251-event database and show in greater detail to what degree the observed features in this subset of events are consistent with the proposed scenario. To assess the sensitivity of space-based imagers for seeing this scenario, we calibrated the absolute responsivity of the THEMIS ground-based imagers. We also show that although not suitable for studies from apogee, IMAGE/FUV imagers can also observe a consistent scenario from a lower altitude. We conclude that in some cases PBIs and subsequent plasma flows can be effective in providing a trigger if the inner magnetosphere is ready to produce a substorm.

Citation: Mende, S. B., H. U. Frey, V. Angelopoulos, and Y. Nishimura (2011), Substorm triggering by poleward boundary intensification and related equatorward propagation, *J. Geophys. Res.*, *116*, A00I31, doi:10.1029/2010JA015733.

1. Introduction

[2] Substorms are large-scale configurational changes in the magnetosphere during which magnetic energy is rapidly converted into particle kinetic energy, some of which is dissipated in spectacular auroral displays. Similar plasma processes are thought to be involved in storing and releasing magnetic energy in magnetospheric substorms and solar flares [e.g., *Akasofu*, 2001]. Unlike the physics of distant phenomena such as solar flares, however, the physics of magnetospheric substorms can be readily investigated by in situ probes. Substorms are a fundamental building block of magnetospheric dynamics. Our understanding of how matter and energy flow through the magnetosphere is incomplete without knowledge of what drives and triggers them. Although much effort has been expended in studying magnetospheric substorms since *Akasofu* [1964] described them, fundamental controversies about their basic physics remain.

[3] It is generally agreed that magnetospheric plasma undergoes reconnection-driven circulation [*Dungey*, 1961]. Driven by the solar wind, plasma on open flux tubes in the polar cap convects in the antisunward direction. In the distant tail, open field lines reconnect again; the resultant closed flux tubes convect sunward within the closed part of the magnetosphere to arrive at the subsolar region. If the polarity of the interplanetary magnetic field (IMF) is southward, magnetospheric flux tubes reconnect with the IMF, open, and convect antisunward again. This circulation and in particular the sunward flow in the magnetotail are not continuous. They are modulated by processes that are not fully understood. Because of inhibition in the flow processes, magnetic energy builds up in the tail during the substorm growth phase [*McPherron*, 1972]. Substorm expansion onset is the sudden, impulsive release of this stored magnetic energy, and the result is the reconfiguration of the magnetosphere back to its quiescent state.

[4] The nature and location of the mechanism(s) that lead (s) to sudden, massive release of stored magnetic energy are controversial. Two main categories of substorm models have been discussed. According to the first model, energy is stored in the intense cross-tail current and associated plasma trapping. Sudden removal of the excess cross-tail current in the inner plasma sheet due to some instability at $<10R_E$ [*Lui et al.*, 1991; *Roux et al.*, 1991] leads to auroral substorm onset and is followed by outward propagation of the activity. According to the second model, the near-Earth neutral line (NENL) model, magnetic flux circulation is enhanced due to the formation of a reconnection line or point in the nightside near-tail at ~20 R_E [*Baker et al.*, 1996]. Ensuing activity propagates inward (toward the Earth) with the auroral signature visible at the ground later.

[5] Although it had many advantages [*Hones*, 1977], the NENL model also had one serious drawback —substorm onsets are almost always observed at relatively low latitudes. In any reasonable average magnetospheric magnetic field model it is very difficult to stretch the magnetic field far enough from the ionospheric region of auroral substorm

[1]Space Sciences Laboratory, University of California, Berkeley, California, USA.
[2]Institute of Geophysics and Planetary Physics, University of California, Los Angeles, California, USA.
[3]Department of Atmospheric and Oceanic Sciences, University of California, Los Angeles, California, USA.

0148-0227/11/2010JA015733

expansion onset to reach to more than 10 R_E at the magnetic equator. Yet, as seen on Geotail, reconnection is almost never observed closer to the Earth than 17 R_E [*Nagai et al.*, 2005], and the probability of occurrence rises rapidly from 20 R_E outward. For this reason the most recent version of the NENL model postulates that the resulting plasma flows propagate inward, causing visible auroral onset when they interact with the inner magnetosphere [e.g., *Shiokawa et al.*, 1997]. This model therefore implies a link between the NENL reconnection event mapping to higher latitudes than the growth phase arc that eventually brightens. Although there were prior reports of high-latitude substorm precursor activity at or near the polar cap boundary followed by equatorward propagation toward the low-latitude onset region, these observations did not give a consistent picture to support the NENL hypothesis.

[6] *Oguti* [1973] made proton and electron auroral observations and showed that an example of an electron aurora that split from high latitudes and moved equatorward. This electron aurora came very close to the low-latitude proton arc and possibly came into contact with it. A breakup then started along the high-latitude boundary of the proton arc at the point of contact or the nearest approach between the two arcs. They observed several other cases of this and called it "contact breakup." *Oguti* [1973] stated that only a relatively few breakups were initiated by such "contact."

[7] Another study that clearly refers to connectivity between the poleward auroral boundary and the auroral substorm onset region was by *Elphinstone et al.* [1995b]. They discussed the relationship between substorm expansion onset and what they called azimuthally spaced auroral forms (AAFs) that appeared prior to onset as seen in the Viking ultraviolet optical data. This activity appeared as an azimuthally spaced (wavelike) intensification in the Viking global images on the equatorward side of the oval covering a large region of local times. From our examination of the images presented in the *Elphinstone et al.* [1995a] paper it seems that the spatial resolution of the Viking imager may have been insufficient to resolve the spatial morphology of the AAFs but according to the paper they were N-S aligned features. According to *Elphinstone et al.* [1995a] these were prevalent at times of high solar wind pressure or negative IMF Bz. *Elphinstone et al.* [1995a] distinguish special AAF substorm onsets in which one of these AAFs brightens forming a substorm bulge. Although the AAFs could cover a large local time region, the substorm bulge was only about 1 h wide in local time. The Viking data showed several other key properties of AAFs and AAF onsets relevant to our discussion. The spatial wavelength of the AAFs prior to substorm onset was between 150 to 600 km. AAFs were found to be substorm onset precursor phenomena occurring prior to intense Pi2 activity and/or substorm associated geosynchronous particle injection. AAFs are located at the equatorward side of the auroral oval, far away and well inside of the open closed field line boundary. Also they stated that coupling via auroral streamers to the high-latitude auroral arc system can sometimes trigger an AAF onset. Thus the PSBL or the open and closed field line boundary may sometimes play an indirect role in substorm onset. They also highlighted the need to compare auroral streamer events with BBF events to determine if a relationship exists between them and whether they have any influence on substorm onsets. They found that several localized activations or pseudobreakups tend to occur following the major onset events. They also observed that in the presence of a double oval it generally takes 5–10 min for the substorm bulge to reach the poleward side of the oval. From this they concluded that assuming that if the poleward part of the double oval is still on closed field lines then the expanding bulge cannot be at the separatrix or at the reconnection site.

[8] Equatorward moving auroral features should map to earthward flowing plasma structures in the magnetotail. In recent years it has become increasingly clear that most Earthward transport of the plasma in the tail takes the form of short duration pulsed plasma flows or bursty bulk flows [*Baumjohann et al.*, 1989; *Angelopoulos et al.*, 1992, 1994]. *Sergeev et al.* [1996] observed bubble-like structures with cross-tail scale sizes on the order of 1–3 R_E in the tail in association with high-speed flows in the expanded plasma sheet. *Henderson et al.* [1998] investigated the relationship between north-south aligned auroral forms observed by the Viking imager and bursty bulk flows.

[9] North-south aligned auroral structures and their association with the substorm has been discussed by *Rostoker et al.* [1987] and *Henderson et al.* [1994] using the Viking auroral imagers. From ground-based auroral observations, *Nakamura et al.* [1993] also investigated how N-S aurora and eastward propagating aurora develop into diffuse and pulsating aurora after the poleward expansion. They also attributed the equatorward expansion of auroral structures to the subsequent earthward transport of plasma from the onset region in the magnetotail. These studies discussed the auroral morphology subsequent to substorm expansion onset during the expansion and recovery phases when the substorm bulge had already expanded poleward. *Henderson et al.* [2002] present a case study of a highly disturbed day (9 November 1998 Kp > 5) when the aurora was extremely bright and showed a double oval configuration. They reported the observation of PBIs with subsequent N-S arcs leading to intensifications near the equatorward boundary. However, none of these prior studies were statistical investigations attempting to establish the frequency of occurrence of such N-S features as precursors to substorm-like reintensifications located at or near a preexisting equatorward E-W arc.

[10] The Time History of Events and Macroscale Interactions during Substorms (THEMIS) mission [*Sibeck and Angelopoulos*, 2008] was designed to provide new opportunities to resolve the "substorm problem." In this program five identical satellites (probes P1-P5) were placed in orbits that permitted probe alignments in the tail so that their instruments could measure in situ particles and fields at various distances along it [*Frey et al.*, 2008]. These probes could make correlated measurements and observe substorm-associated electric and magnetic field and plasma properties, and from the timing of the changes infer the direction of propagation. A main goal of THEMIS is to identify the location and time of origin of a substorm in the magnetosphere and compare that time to the substorm auroral intensification. The probes were supplemented by a set of 21 ground-based observatories (GBO) in North America that documented auroral configuration [*Donovan et al.*, 2006; *Mende et al.*, 2008]. At each site, there is an all-sky imager (ASI) and a magnetometer. This observatory network pro-

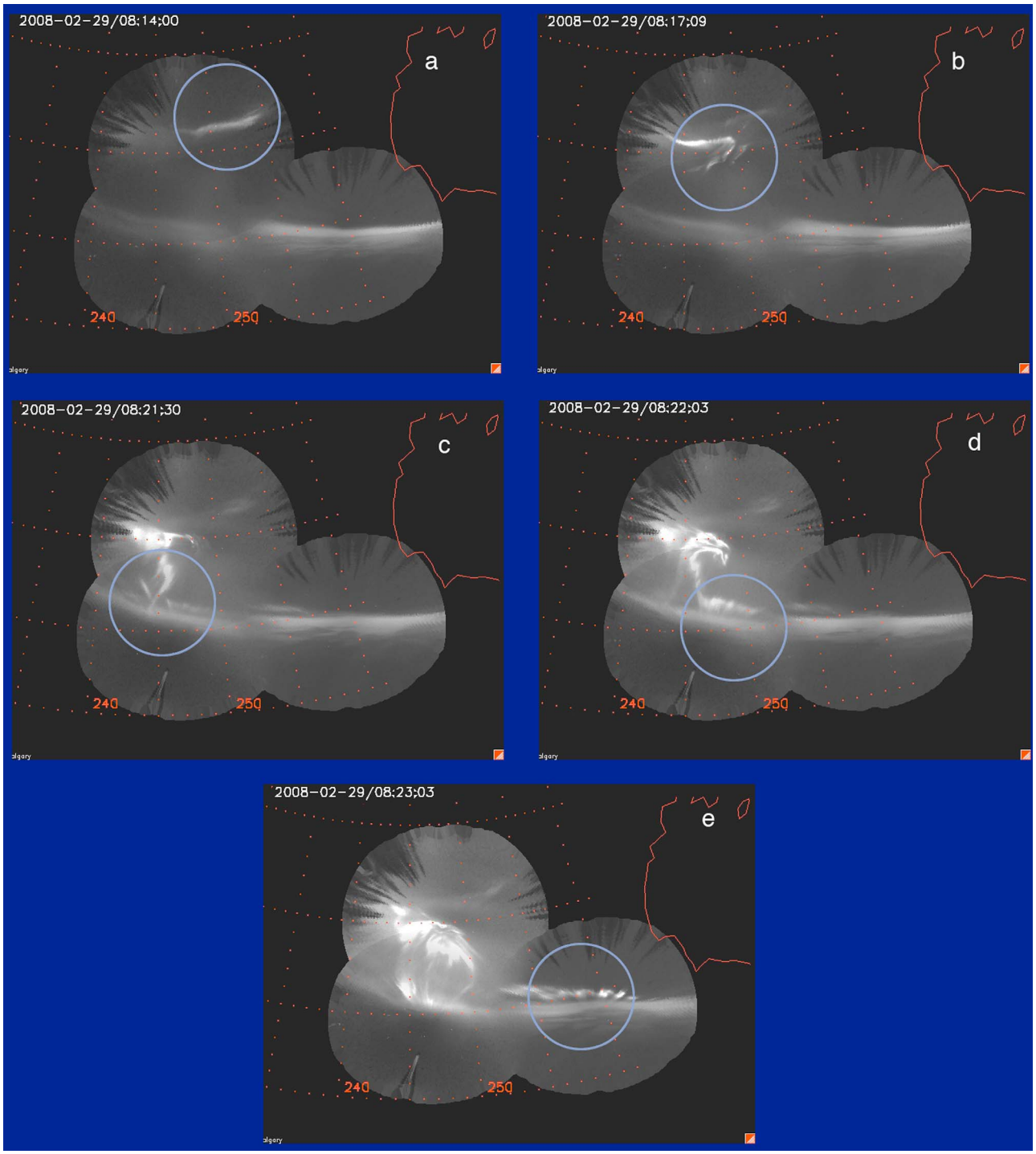

Figure 1. Collage made by the mosaic software from the data in the example event from *Nishimura et al.* [2010].

vided unprecedented coverage rivaling that of satellite-borne imaging combined with high spatial and temporal resolution (3 s cadence of images and 2 Hz of magnetic measurements) and sensitivity attainable only from the ground. Most importantly, the multistation camera chain was able to monitor high-latitude regions over a range of longitudes close to and far from onset longitude.

[11] *Kepko et al.* [2009] reported observations of substorm precursor activity poleward of the expansion onset location (630 nm redline activity measured by special monochromatic imagers). The red line was presumably produced by soft electron precipitation, which corresponded to high-latitude, equatorward propagation of the aurora immediately prior to substorm onset on the onset meridian. Simultaneously P4 and P5 observed strong Earthward flows at and after substorm onset.

[12] *Nishimura et al.* [2010] presented a new set of THEMIS GBO observations of the night side aurora. They

Table 1. The Results of the *Nishimura et al.* [2010] Statistical Study From 251 Cases

Category 1	Category 2	Category 3	Category 4
212	26	12	1
84%	10%	5%	0.5%

analyzed 251 events and reported that a distinct, repeatable sequence of events leads to substorm onset. The sequence starts with a poleward boundary intensification (PBI) typically away from the meridian of the onset and is followed by a north-south (N-S) aligned arc or patch moving equatorward toward the onset latitude. When mapped to the magnetotail, a N-S auroral motion presumably represents an earthward flow. The flow appeared to start at the PBI, presumably at the open-closed field line boundary, and ended at the inner magnetospheric region where the near-Earth substorm instability and auroral breakup commence. On average, substorm onset was delayed by about 5.5 min relative to PBI onset.

[13] *Nishimura et al.* [2010] presented three detailed examples out of the 251 events examined. From a statistical analysis they stated that 84% of the substorm cases show patterns consistent with the sequence described above. This seemed highly unlikely considering the difficulties involved in the observations, including clouds and data gaps. If this were true then this would imply that almost all substorms would exhibit this behavior and almost all substorm commencements must be associated with PBI-induced triggering. Another important issue is that they did not separate substorm onset, substorm reintensifications or pseudobreakups in their paper.

[14] Both *Kepko et al.* [2009] and *Nishimura et al.* [2010] highlight the role of equatorward propagating auroral features immediately prior to substorm onset. *Kepko et al.* [2009] studied a single case; *Nishimura et al.* [2010] performed a statistical study in addition to describing the three cases. The *Nishimura et al.* [2010] scenario places a large emphasis on the PBI, suggesting that a sudden plasma injection across or at the open-closed boundary initiates that phenomenon. The results of both of these studies have significant implications for our understanding of substorms. Is a PBI a ground-based signature of an NENL formation or an enhancement in Distant Neutral Line (DNL) reconnection? Is an equatorward propagating N-S aurora the missing link required to connect far-tail reconnection events to the near earth region at substorm auroral break up? Is the described scenario a fundamental part of the substorm process or one of many possible trigger mechanisms that can destabilize the magnetotail?

[15] Because of the significance of these observations we revisited 20 randomly selected cases of the Nishimura et al. list of 251 events. We have obtained mosaic image sequences of all 20 cases, enhancing those features that were most relevant to the crucial auroral evolution signatures and compared our results with the *Nishimura et al.* [2010] study. Coauthors S. B. Mende and V. Angelopoulos contributed to the *Nishimura et al.* [2010] study by making the THEMIS data available to Nishimura and collaborators and Y. Nishimura contributed to this paper only by providing the list of the 251 cases. The two analyses were performed independently by different persons. In addition, we searched the IMAGE satellite UV image database for events that would show signatures consistent with the above mentioned preonset activities.

2. Data Set and Analysis

[16] To conduct a study in a truly independent fashion, we used a random number generator to select our 20 events from the event list provided by our coauthor Y. Nishimura. We used independent tools for image processing, ionospheric projection and auroral intensity matching across image boundaries and produced mosaic movies for all the cases we studied. The mosaic movie software used in our study works backward; it selects a pixel of the output image

Table 2. Tabulation of the 20 Randomly Selected Events From the *Nishimura et al.* [2010] List

	YYYYMMDD	HHMM	Station	Category 1	Category 2	Category 3	Category 4	Class 1 N-S = 2	Class 2 E-W = 1	Class 3 No = 0
1	20071210	618	fsim	1						1
2	20071212	1027	fykn				1	1		
3	20080107	832	fsim	1				1		
4	20080108	446	fsmi	1					1	
5	20080114	411	gill	1						1
6	20080124	706	fsmi	1					1	
7	20080201	1113	whit	1				1		
8	20080202	812	fsim	1				1		
9	20080202	902	gako	1				1		
10	20080210	437	kuuj	1						1
11	20080220	547	gill	1				1		
12	20080301	359	snkq	1						1
13	20080306	722	yknf			1				1
14	20080314	633	gill	1				1		
15	20080315	1013	kian		1			1		
16	20080323	707	fsim		1					1
17	20080327	727	tpas	1					1	
18	20080329	711	fsim		1					1
19	20080401	556	gill		1				1	
20	20080409	1001	fykn	1				1		
				14	4	1	1	9	4	7
				70%	20%	5%	5%	45%	20%	35%

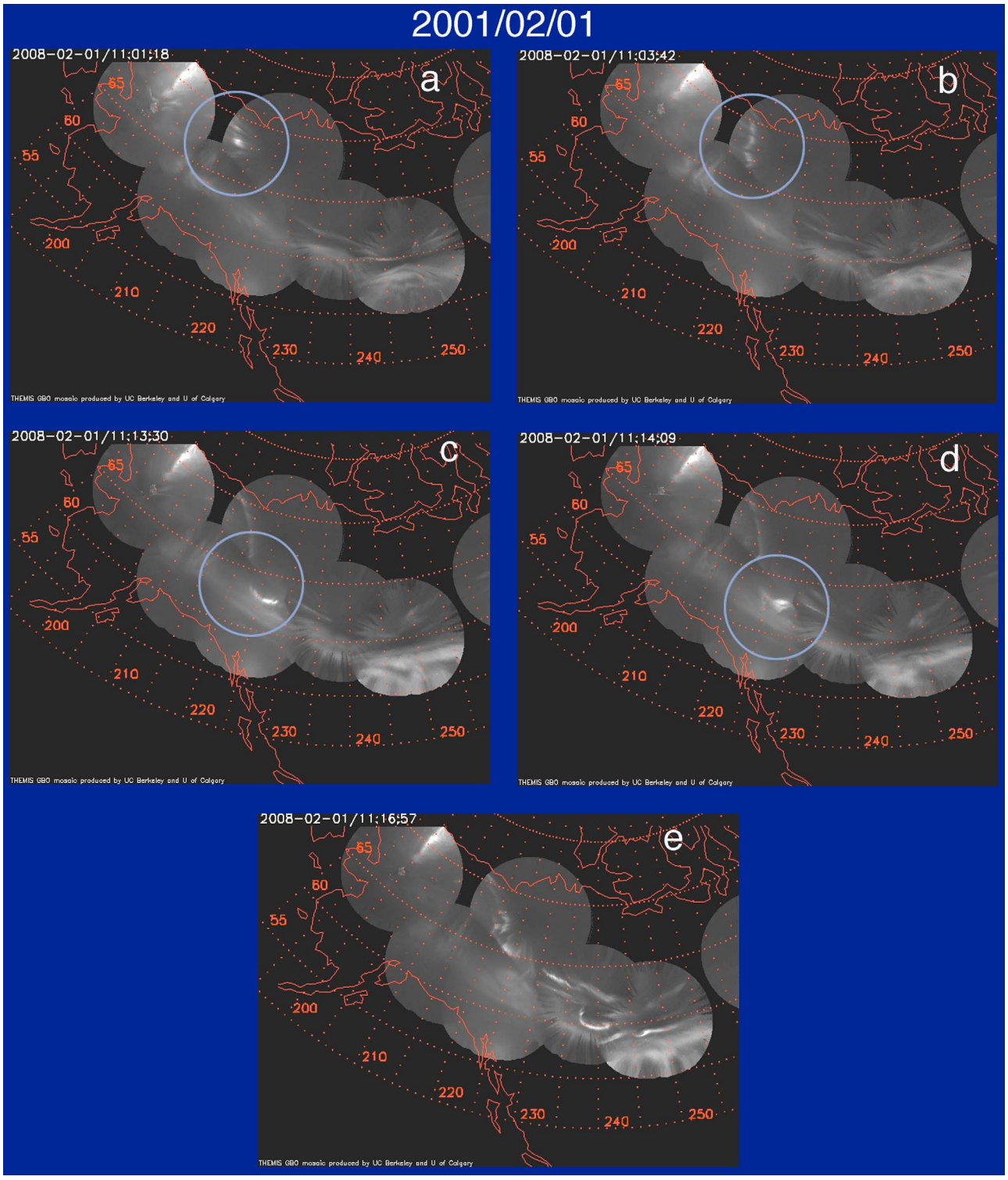

Figure 2. Event collage for 1 February 2008 event. Blue circles indicate regions of interest.

matrix described by its Cartesian coordinates corresponding to a latitude and longitude point on the mosaic and finds the corresponding image point in the field of views of each appropriate camera that may contribute to that location. Once these points are found, it fetches the pixel intensity from each contributing camera and takes a weighted average of the intensities of the image point from each relevant station. For weighting it uses the inverse distance between the station location and the output pixel location. This ensures that the pixel weighting is inversely proportional to the distance to the station, that pixels receive their intensity predominantly from the closest station, and that there is a

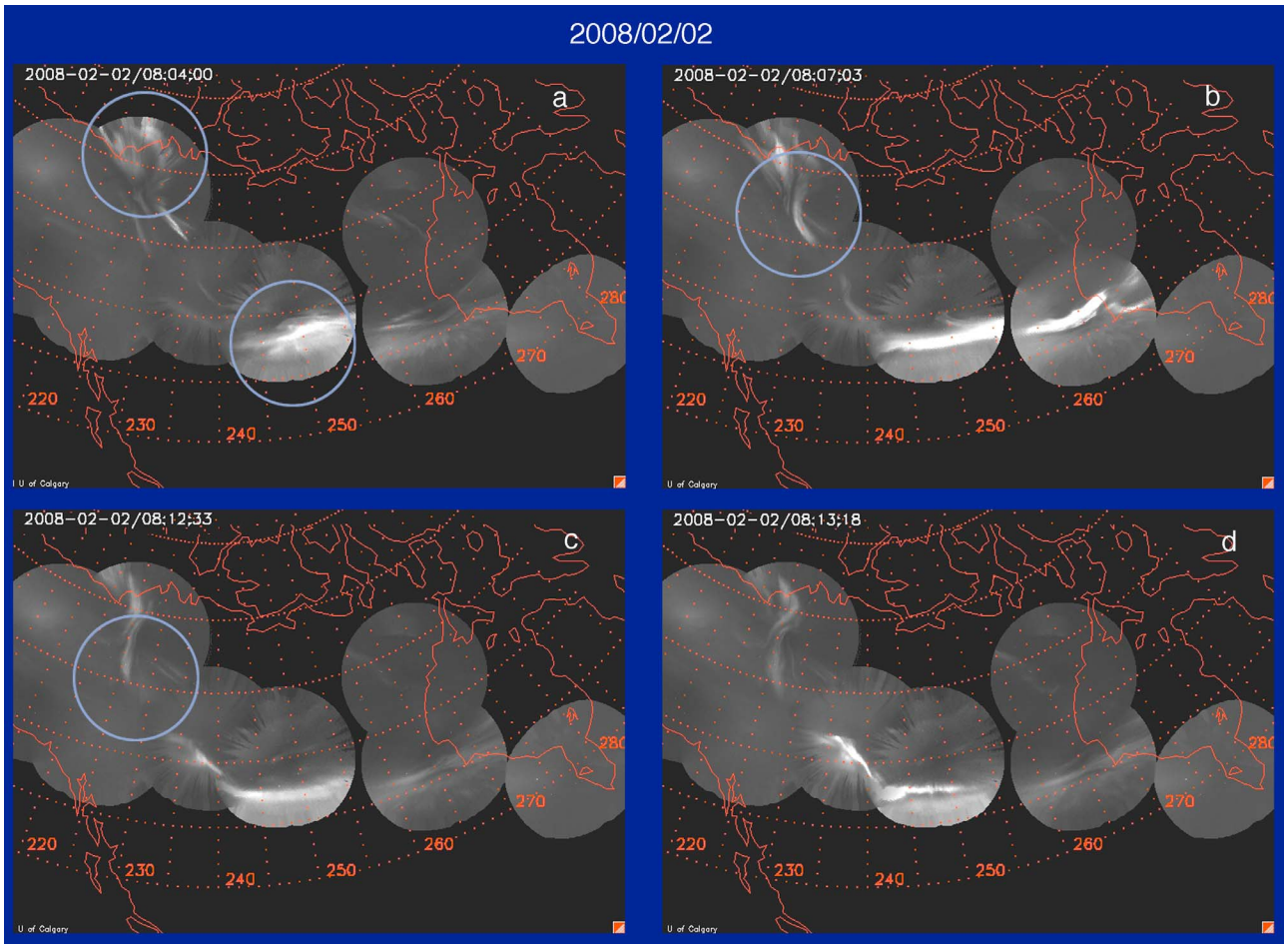

Figure 3. Collage for 2 February 2008 event.

smooth transition between adjacent stations in the overlapping regions of their field of view (FOV). One feature of the software is that all the mapping functions $x_i = f(n, x_o, y_o)$ and $y_i = g(n, x_o, y_o)$ and the weighting factor $w(n, x_i, y_i)$ can be worked out only once for the fixed geometry of the entire array. Tables are made from the functions so that each can be read rapidly during routine processing. In the functions above, x_i and y_i are the pixel coordinates in the camera frames; n is the station designator; and x_o and y_o are the Cartesian coordinates of the pixels in the output latitude-longitude mosaic image.

[17] *Nishimura et al.* [2010] showed the event that occurred on 29 February 2008 at 08:22 as typical. We reproduced 5 frames of the mosaic from the event in Figure 1 to emphasize the most important features in their study. An auroral intensification at relatively high latitudes occurred at 08:14 (Figure 1a). As this was close to the polar cap boundary it is interpreted here as a poleward boundary intensification. By 08:17:09 this intensification moved slightly equatorward, developed a NE to SW fold (Figure 1b), and expanded further equatorward until it intercepted the E-W arc at 08:21:30 (Figure 1c). The preexisting arc and the NS arc seemed to connect at 08:22:03 (Figure 1d), and an intense rayed aurora was seen at 08:23:03 (Figure 1e). This type of aurora just poleward of a preexisting E-W arc is a typical onset signature [*Mende et al.*, 2009]. After onset the aurora intensified and rapidly expanded poleward. It is interesting that this onset point is not on the same meridian as the PBI. Meridian-scanning photometers or a chain of all-sky imagers located on the substorm onset meridian would have missed the PBI and associated events entirely.

[18] *Nishimura et al.* [2010] presented other case studies in which this pattern is observed. To be able to observe PBI events at a different latitude and longitude from the substorm onset point requires a large array of cameras and clear skies at several key camera stations. Unfortunately, conditions are rarely good enough to document the entire process, as in Figure 1. To facilitate a significant statistical study using only one winter of data, it is necessary to assume that catching only parts of the sequence described in Figure 1 is sufficient as long as they are consistent with the described process. *Nishimura et al.* [2010] made that assumption, and we do the same.

[19] *Nishimura et al.* [2010] took 251 onset events from the period between 10 November 2007 and 29 April 2008 and made mosaic movies of the precursor activities using data from stations at which the sky was reasonably clear. They reviewed the imagery and divided the activities into four categories according to the following considerations (we use their definitions): (1) A new N-S and/or E-W arc

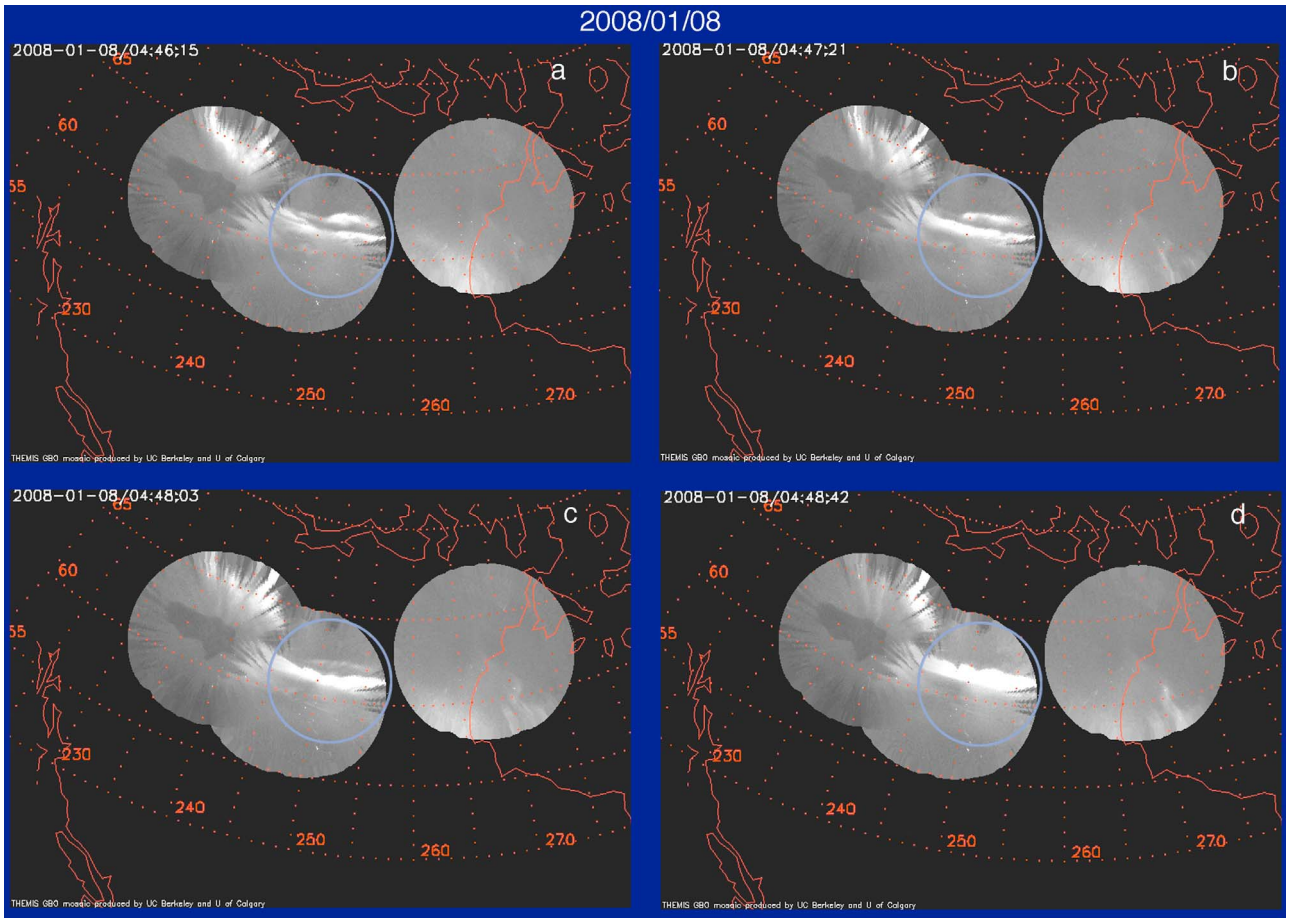

Figure 4. Collage for 8 January 2008 event.

reaches onset location just before an auroral onset is observed; (2) No newly formed N-S or E-W arc is seen moving toward onset location, but the preexisting growth phase arc exhibits structured forms moving along the arc. Note that a sudden (generally equatorward) shift in the location of the preexisting arc is seen just before auroral onset; (3) No precursor activity except faint growth phase arcs is detected in available imager FOVs; and (4) Other complex events.

[20] Recognizing that coverage was usually inadequate to see the entire process starting with the PBI, it appears that in their statistical study *Nishimura et al.* [2010] focused mainly on the last part of the scenario illustrated in Figure 1, the interaction of the preexisting E-W arc with other auroral forms. For example, they mention that in many cases N-S auroral forms were observed to first propagate equatorward getting near the preexisting E-W arc. They then turned into an E-W auroral form that traveled parallel to the earlier E-W arc and merged with it to initiate substorm intensifications at a different longitude. The new E-W arc merging with the old at the onset location was included as *Nishimura et al.* [2010] category 1 because they imply that in many cases coverage was insufficient to observe the entire sequence, and it was only possible to observe this last phase.

[21] We reproduced their results in Table 1.

[22] *Nishimura et al.* [2010] placed 84% of the cases in category 1 (a new N-S and/or E-W arc reached onset latitude just before observation of an auroral onset). In our opinion, this high percentage may be due to the mixing up of several different types of events. It was important to differentiate between newly reported PBI-derived N-S structures at substorm intensification onset and E-W events consisting of the consolidation of two E-W auroras. The latter ones could often have different origins. Substorms starting off with interactions of several preexisting E-W arcs have been commonly observed. Thus, observations of two E-W arcs merging cannot be regarded as evidence for the PBI and subsequent N-S auroral process reported in case studies such as shown in Figure 1. We introduce a new categorization that divides the events into 3 classes:

[23] 1. Category N-S with PBI (or at least some equatorward propagating N-S feature) which, when getting close to the break up arc latitude, appears to initiate breakup within ~1 min. It should be noted that observation of the intersection of the N-S feature with the E-W arc before onset commencement is not necessarily proof that the entire scenario initiated by a PBI has actually played out.

[24] 2. Category E-W in which two E-W arcs are seen. The poleward arc drifts equatorward, and when they meet, substorm breakup and subsequent poleward expansion occur.

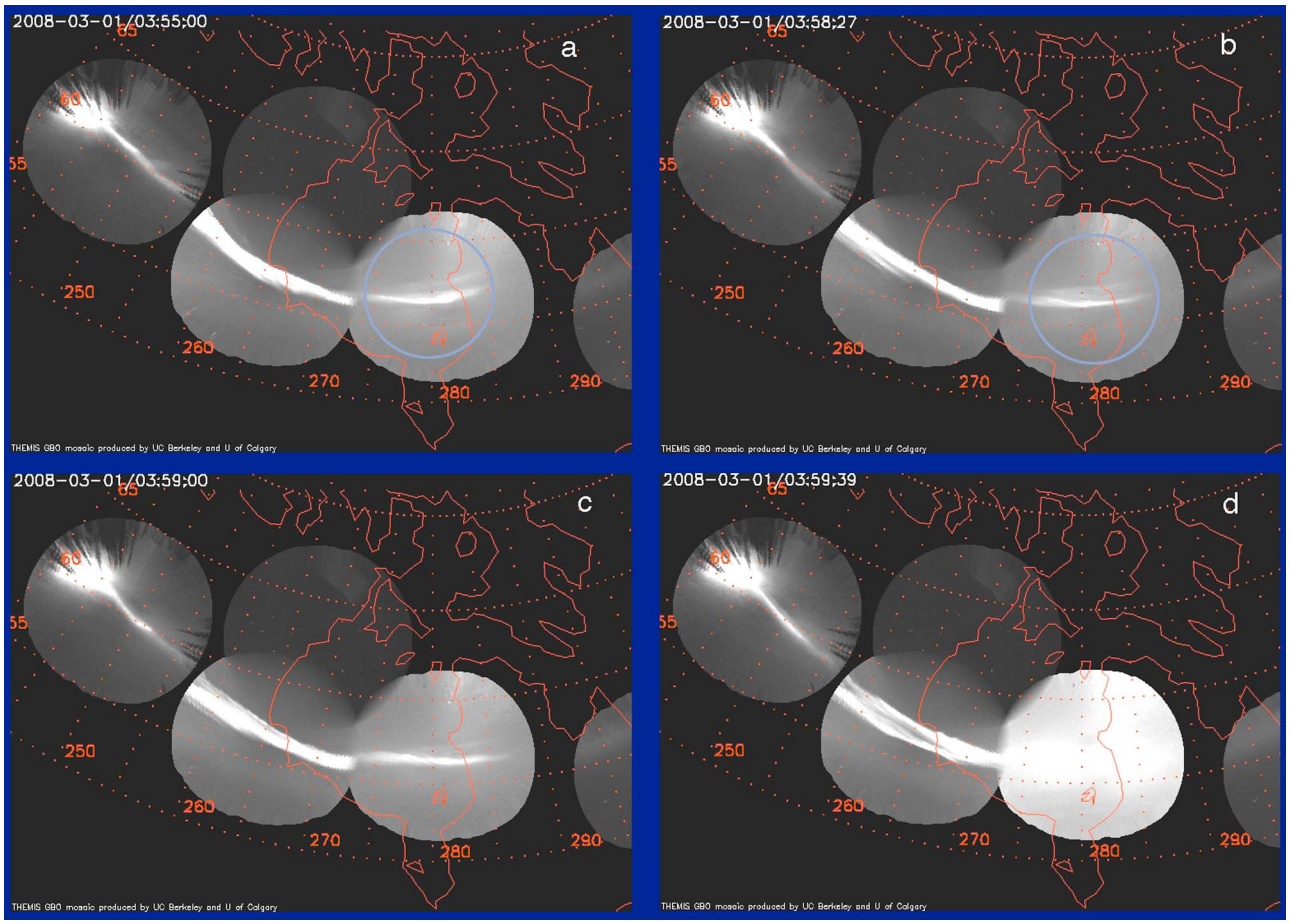

Figure 5. Collage for 1 March 2008 event.

[25] 3. Definitely not consistent with the PBI-initiated scenario or cases in which it is impossible to make a unique identification due to a recent substorm poleward expansion that had left residual high-latitude auroras scattered.

[26] Our 20 cases are given in Table 2. Columns 5 to 8 show the *Nishimura et al.* [2010] categorizations and columns 9 to 11 our classifications. The bottom row shows overall averages for the 20 case samples. According to the *Nishimura et al.* [2010] categorization, 70% of this particular subset was in Category 1. In our classification scheme 45% showed N-S-propagating features that resulted in a Class 1 designation and 20% showed only E-W features. Since *Nishimura et al.* [2010] counted our first two classes as a single category, the combined percentage was 65% (compare with their 70%). We regard this as valid comparison of the two different techniques. We note, however, that only our class 1 shows the clear signature of equatorward propagating N-S features as in Figure 1. In our opinion our class 2 onsets are most likely to be consistent with other previously documented causes rather than the PBIs and related phenomena reported by Nishimura et al. East-West arcs are standard features of presubstorm auroras appearing simultaneously at high and low latitude and at times forming double ovals [*Elphinstone et al.*, 1995a; *Pulkkinen et al.*, 1995; *Gjerloev et al.*, 2008]. The contacting of two E-W arcs at substorm onset has been reported [e.g., *Kornilova et al.*, 2006]. We should also note that it is difficult to unambiguously observe contacting of two parallel arcs unless they are viewed exactly at the magnetic zenith. Thus we feel justified in separating the events associated with E-W arcs into a separate category.

[27] Four rows of Table 2 are noted. Events 7 and 8 are put into class 1 with N-S auroral features. Event 4 shows E-W arcs we put into class 2. All three events were graded by *Nishimura et al.* [2010] as category one. Although event 12 was graded as category 1 by *Nishimura et al.* [2010], our study showed it to be in class 3. Below we present a case-by-case discussion of these four events to illustrate the differences and similarities.

[28] Figure 2a shows the auroral situation at 11:01:18 with the preexisting E-W arc stretching from longitude 210 to 260 degrees. The blue circles indicate a bright intensification. This quasi N-S (more precisely, NW-SE) feature expands and develops between 11:03:42 and 11:13:30 (Figures 2b and 2c). Note that although the NW-SE feature is clearly seen in Figure 2b, it ends abruptly at the edge of the FOV of the lower station. This indicates a likely sky obscuration there and that the feature in reality was most likely extended more equatorward. We can assume that it was continuous in the lower-latitude camera, and it actually touched the E-W arc at 11:13:30 (Figure 2c). Onset started at 11:14:09 with brightening in Figure 2d. Thus, the interaction between the

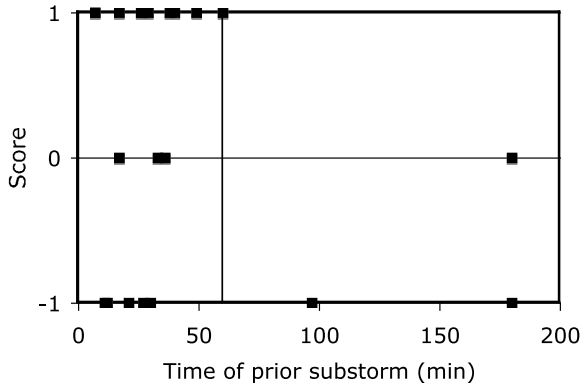

Figure 6. The distribution of the 20 substorms according to the time elapsed since a substorm onset. Categories 1, 2, and 3 had scores of 1, 0, and −1, respectively.

NW-SE feature and the E-W arc occurred further west than the brightening at 11:14:09 (Figure 2d). Figure 2e shows a typical image after substorm expansion onset. Although lack of high-latitude data may have prevented us from observing the true onset of the PBI, this example is consistent with the *Nishimura et al.* [2010] observations of N-S auroral propagation from higher latitude. We therefore graded it as a Class 1 event.

[29] Figure 3a shows the auroral situation at 08:04:00 with the preexisting E-W arc most clearly seen at Fort Smith between 240 and 255 degrees geographic longitude. There is also auroral intensification at much higher latitude in the Alaska region, also indicated by a blue circle at longitude 220 degrees. From 08:07:03 to 08:12:33 there is distinct activity and equatorward propagation in the form of NW-SE features shown in Figures 3b and 3c. It seems that the station Whitehorse (marked as WHIT in Figure 3c) is obscured because the westward continuation of the E-W arc is not seen there. Interaction between the southward moving features and the E-W arc is obscured at Whitehorse. At 08:13:18, however, the activity culminates in substorm expansion onset (Figure 3d) a little eastward of the presumed interaction of the two types of auroras. Although we did not see the "cradle-to-grave scenario" of PBI to substorm intensification onset, the morphology could be consistent with it. Therefore, we gave this event also a class 1 classification.

[30] The second of February 2008 was very active, however, three substorms, which occurred at 07:45, 08:12, and 08:37 UT, were analyzed elsewhere [*Mende et al.*, 2009].

[31] Figure 4a shows the auroral situation at 04:46:15 (Figure 4a) with 2 parallel E-W arcs in close proximity. At 04:48:03 (Figure 4c) the poleward arc fades and appears to move equatorward. At the same time the equatorward arc intensifies. It is difficult to say whether the merging of the two arcs as seen at 04:48:42 (Figure 4d) was the result of the poleward arc moving south, the apparent northward motion of the southern arc, or both. The net result is that the arcs merged at this point.

[32] This merging of the two parallel arcs can be regarded as consistent with the last stages of the scenario starting with the PBI, followed by equatorward propagation and the azimuthal development of a parallel arc that then merges with the preonset east-west arc. We believe that this is why the case was put into the first category by *Nishimura et al.* [2010]. Within the available images, however, we did not see any indication of a N-S structure, and merging of the two parallel east-west arcs is an often observed substorm feature regardless of whether PBIs or anything else is observed. Therefore, it was important to keep them as a separate class, and we rated this as a class 2 event.

[33] Figure 5a shows the situation at 03:55:00 with the E-W arc extending from 240 to 285 degrees longitude. At station SNKQ (longitude of 280 degrees), we see a second E-W arc slightly poleward. At 03:58:27 (Figure 5b) the region between the two E-W arcs is filled with faint aurora. At 03:59:00 (Figure 5c) the poleward arc fades out and the aurora hugely intensifies at SNKQ at 03:59:39 (Figure 5d), signifying substorm intensification onset.

[34] Because we found it difficult to classify this event to support the scenario given by *Nishimura et al.* [2010], we ranked it as a class 3 event. This event was listed by *Nishimura et al.* [2010] as a category 1 event. Presumably they regarded interaction of the two E-W arcs as supporting their scenario.

[35] In summary, these examples illustrate the difficulties involved in classifying these events. Granted that the coverage even with the extensive GBO instrumentation is very rarely good enough to observe the entire nightside oval, we cannot expect to have perfect documentation of a substorm scenario every time. We propose that seeing some N-S feature propagating equatorward and interacting with the preexisting E-W arc followed by an equatorward arc breaking up and intensifying and undergoing poleward expansion is a sufficient marker of this type of event. The interaction of two E-W arcs is a common occurrence reported many times before, and it cannot be regarded as a unique signature of the scenario that begins with PBIs. It was therefore reasonable to divide the sample into two categories.

3. Substorm Occurrence Frequency

[36] In most classical substorm studies it is assumed that substorms occur after a prolonged, relatively quiet growth phase. During this phase the magnetosphere acquires energy by magnetic field configuration change, and this energy is released in the substorm. Most classical substorm studies therefore tend to use so-called self-standing or "isolated substorms." The recovery phase of a prior substorm may finish in less than an hour, in which case the next substorm can also be called an isolated substorm. However, as far as we know, no such selection criterion was applied in the *Nishimura et al.* [2010] study. As an arbitrary rule of thumb, an isolated substorm can be one that occurs at least 1 h after a substorm. It is instructive to ask what statistical rate of occurrence was associated with the substorm sample used in these studies.

[37] The 20 randomly selected cases from the *Nishimura et al.* [2010] list provide another important clue. On the THEMIS GBO substorm list (ftp://justice.ssl.berkeley.edu/events/), we found substorms that occurred just prior to the events shown on the Nishimura list. We plotted the difference between the onset times in Figure 6. The vertical line at 60 min is a reference line for 1 h. On the right of the line, events on the Nishimura list can be regarded as isolated substorms. All substorms that clearly show the *Nishimura*

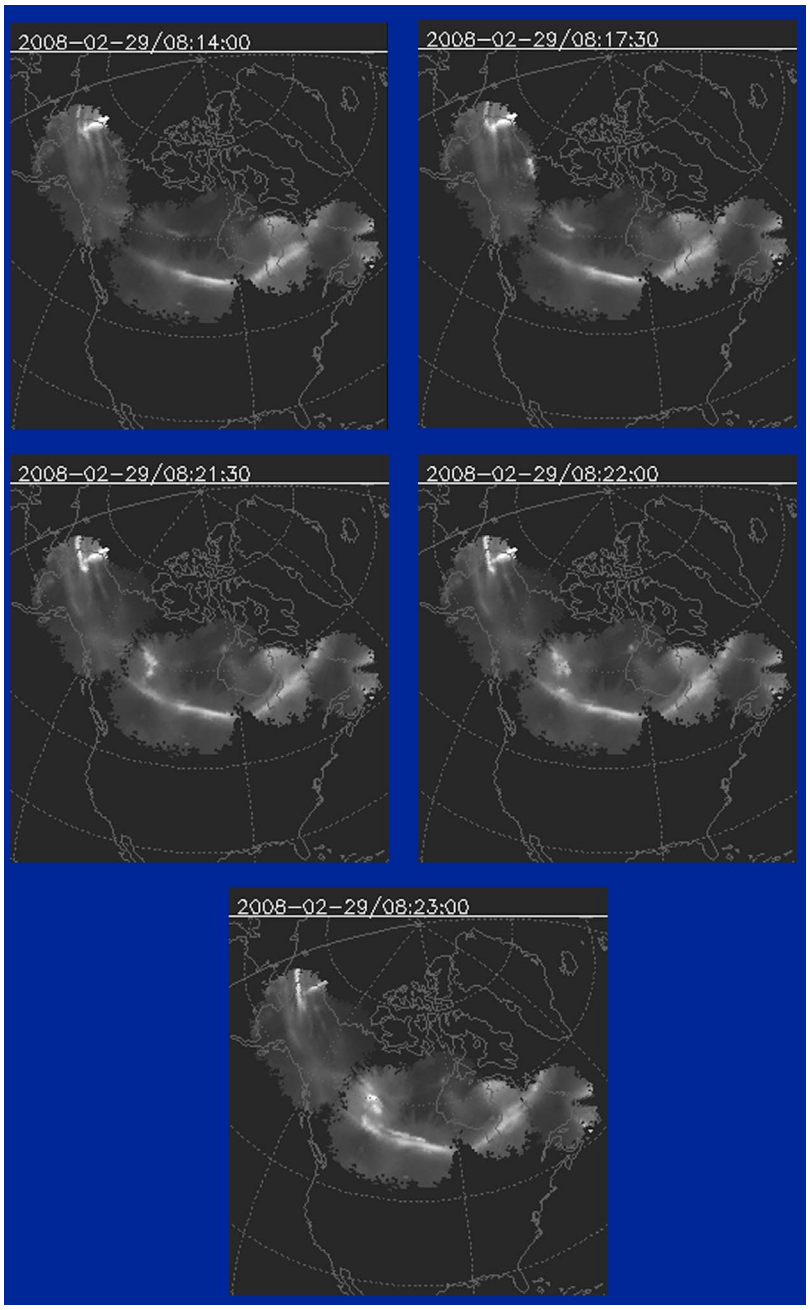

Figure 7. Simulation of what IMAGE would have seen from 20,000 km altitude if it had seen the event on 29 February 2008 described by *Nishimura et al.* [2010] .

et al. [2010] pattern are intensifications, not isolated substorms as defined by our 1 h limit.

4. PBI-Related Substorm Observations With the IMAGE Satellite

[38] Cloud cover poses a major difficulty in obtaining statistically significant observations of PBI-triggered substorm intensifications from ground-based all-sky images. It is rare to have clear weather over a large enough area of the auroral oval to be certain that some precursor PBI activity and associated equatorward propagating auroral forms occurred. Space-based imagers, such as the wideband imaging camera (WIC) on the NASA IMAGE satellite [*Mende et al.*, 2000], have often covered the entire auroral oval and were unaffected by clouds. Therefore, a study of the data taken from space-based auroral imagers should have produced unquestionable statistics about the frequency of occurrence of PBI-triggered substorm intensifications. Why are there no reports of such events from the large body of space-based optical data?

[39] To answer this question, we needed to determine whether these space-based cameras were sensitive enough to see typical PBI-associated auroras. We first measured the absolute intensity and spatial extent of such auroras. Then, using the measured intensity and spatial extent, we modeled

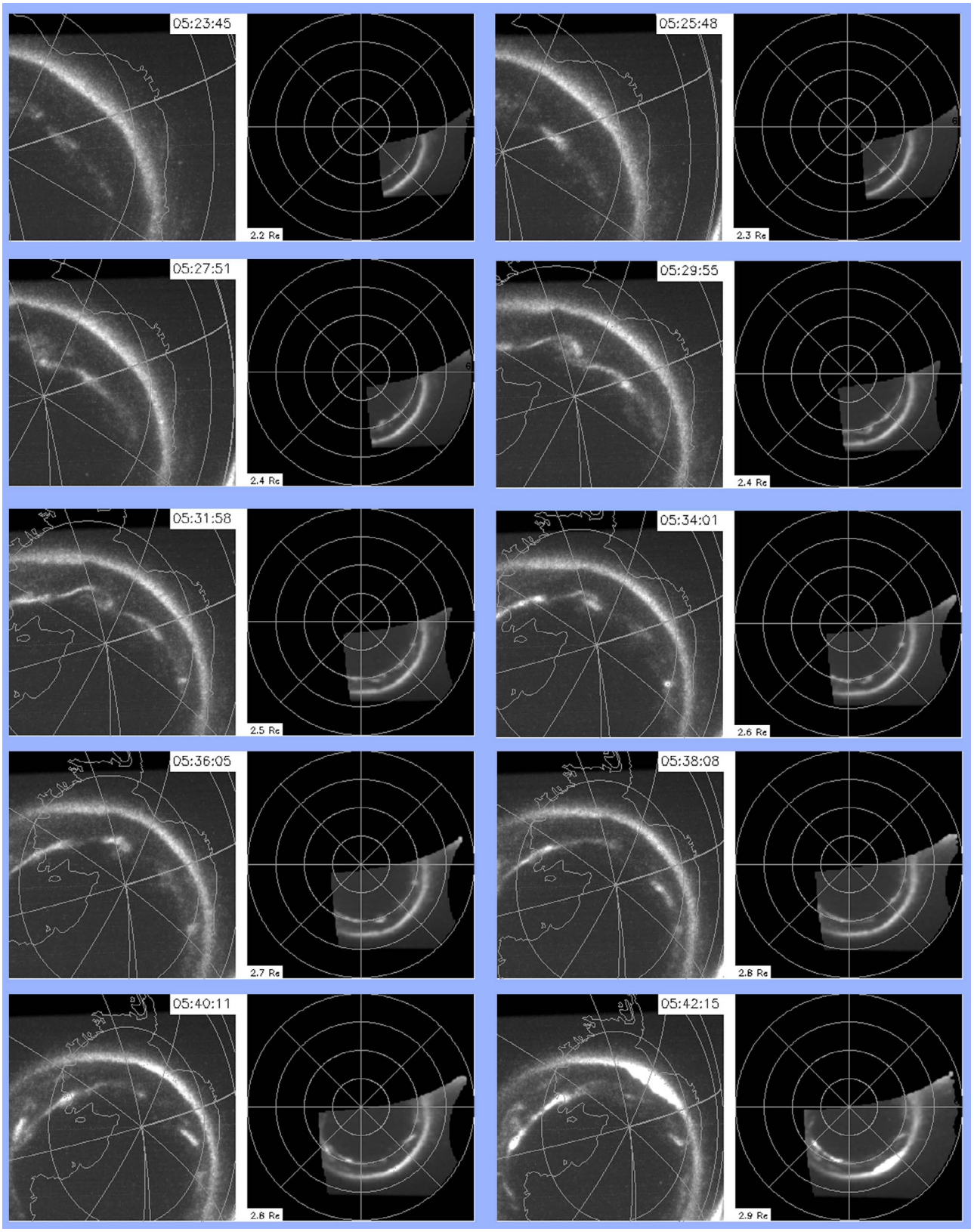

Figure 8. Substorm onset observed by IMAGE when satellite altitude was between 7600 and 12000 km on 3 July 2003. (left) The image of each element of the collage is the actual image seen by the WIC, and (right) also shown is the same image projected on a magnetic latitude local time grid.

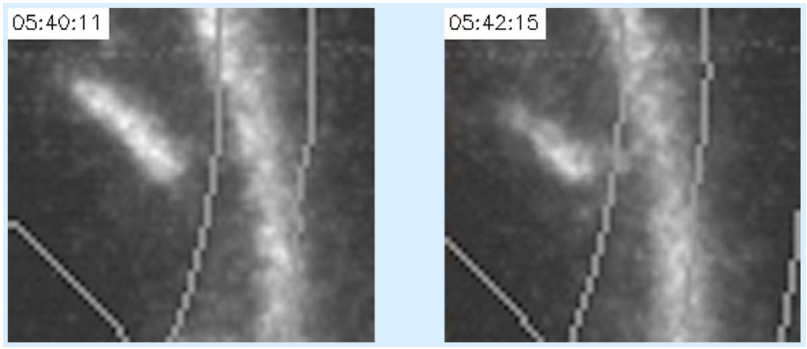

Figure 9. Detail from the two WIC images in Figure 8 (bottom). A substorm occurs between 05:40:11 and 05:42:15. There is a faint but discernable bridge between the poleward feature and the preexisting arc.

the response of WIC and estimated its response to an aurora of the same intensity and spatial extent.

[40] We discuss calibration of the THEMIS ASIs in Appendix 1. Based on this calibration, we converted the ASI images for the *Nishimura et al.* [2010] prime event (29 February 2008) into absolute intensities. We used the data to build a model to display them in perspective and applicable image quality as if they had been viewed by IMAGE WIC from 20,000 km altitude. In calculating the signal strength of the intensity display, we assumed that the mean energy of the precipitating electrons was 5 keV and thus used the 377 AD units per erg cm^{-2} s^{-1} of precipitated energy as given for IMAGE WIC [*Frey et al.*, 2003, Table 4].

[41] An image collage produced from representative images is given in Figure 7. The images were taken at the same time as the images used in Figure 1. From Figure 7 it appears that when the IMAGE satellite was at less than 20,000 km altitude, the WIC of the IMAGE FUV system would have had the resolution and sensitivity to see the event reported by *Nishimura et al.* [2010] and discussed earlier in this paper.

[42] Because IMAGE was in a highly eccentric orbit, getting this perspective was serendipitous. IMAGE spent most of its observing time at 7Re or 40,000 km altitude with a pixel corresponding to about 60 × 60 km at ground level. Under those conditions it is very difficult to make the required observations. At altitudes of 20,000 km or less, the satellite is moving rapidly in the radial direction and to capture substorm onset exactly at the right point in the orbit was a rare occurrence.

[43] On 3 July 2003 when the satellite was at an observing range of fewer than 12,000 km and traveling away from the Earth, we got an excellent perspective viewing of a substorm onset. This event is presented in Figure 8. The collage consists of ten image pairs covering a time range from 05:23:45 to 05:42:15 (K_p = 3). The left image of each pair is the actual image seen by the WIC, and the right image is the image projected on a magnetic latitude/local time grid. In the last frame (05:42:15) we can clearly see that substorm onset took place. The bright aurora shows the classical onset enhancement of a preexisting equatorward arc and initiation of poleward expansion. In this work we are more interested in the poleward boundary and its presubstorm intensifications. The first poleward boundary intensification is observed in the 05:25:48 frame at the longitude region in which onset would later take place. A very small intense spot develops from 05:31:58 to the following frame (05:34:01) at 70 degrees magnetic latitude and about 04:30 MLT. This very bright, tiny spot is most noticeable in the actual WIC image. It marks the approximate location of the feature that can be seen very clearly in frame 05:40:11 at about the same location. In this frame it appears separate from the long preexisting E-W substorm arc. In the next frame (05:42:15), the same feature is a little fainter, but one can just make out a bridge between the feature and the E-W arc. The appropriate regions from these two images in Figure 8 (bottom) were enlarged and reproduced in Figure 9, which clearly shows a faint auroral bridge between the two features in the right image with onset at 05:42:15. (This bridge did not exist on the previous frame (05:40:11) as shown in Figure 9 (left).) The morphology of this event is consistent with a precursor PBI and associated equatorward moving features as reported by *Nishimura et al.* [2010]. Unfortunately, because of the poor time resolution (2 min cadence) of the IMAGE data, it is impossible to learn the relative timing of the various features and the substorm onset. We know that IMAGE WIC took a 10 s exposure about every 2 min, and the image taken at 05:42:15 is a 10 s snapshot containing both equatorward coupling from the PBI and substorm expansion in a rather fully developed stage., This suggests that either the "bridge" precursor stayed in place during the early (<2 min) part of substorm onset or onset started first and the "bridge" signature followed after.

[44] This could be an example of a PBI and associated activity (bridge) far enough away in longitude from the onset meridian that it would be easy to miss them with a network of meridionally located, ground-based observatories. Furthermore, it should be noted that the IMAGE satellite was in a rare favorable position because the substorm occurred while the satellite was at an altitude of less than 12,000 km (i.e., relatively near perigee on its elliptical orbit) and rapidly moving away from the Earth. Despite the favorable circumstances, it was still difficult to detect the key feature connecting the PBI and the E-W arc.

5. Discussion

[45] We conclude that PBIs and associated equatorward propagating auroral forms can regularly (but not always)

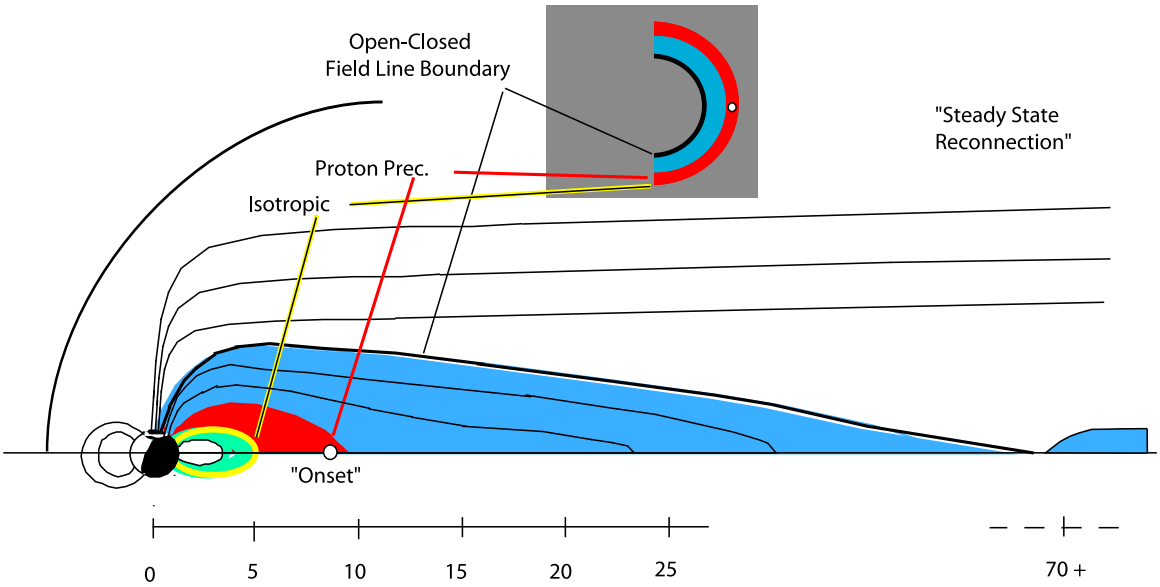

Figure 10. Sketch of the nightside configuration of the quiescent magnetosphere. From inside out, region of trapped protons (green), isotropic boundary (yellow), region of precipitating protons (red), closed field line region containing diffuse electron and weak protons auroras (blue), and the open-closed field line boundary (black line). The top right illustration is a schematic view of the nightside northern polar region.

trigger substorm-like sudden intensifications and characteristic poleward expansions in the aurora. It is equally important to note that not all substorms are triggered this way. Thus, we propose that PBI intensification and subsequent equatorward traveling plasma flows are just one of several possible substorm triggers. The importance of poleward boundary events and subsequent equatorward propagation causing "contact breakup" and subsequent substorm intensification was noted by *Oguti* [1973]. Quoting from *Elphinstone et al.* [1995a, p. 7966] states "… coupling via auroral streamers to the high-latitude auroral arc system can sometimes trigger an AAF onset. Thus the PSBL or the open and closed field line boundary may sometimes play an indirect role in substorm onset." If we were to read N-S arcs instead of auroral streamers, PBIs at the open closed field line boundary instead of high-latitude

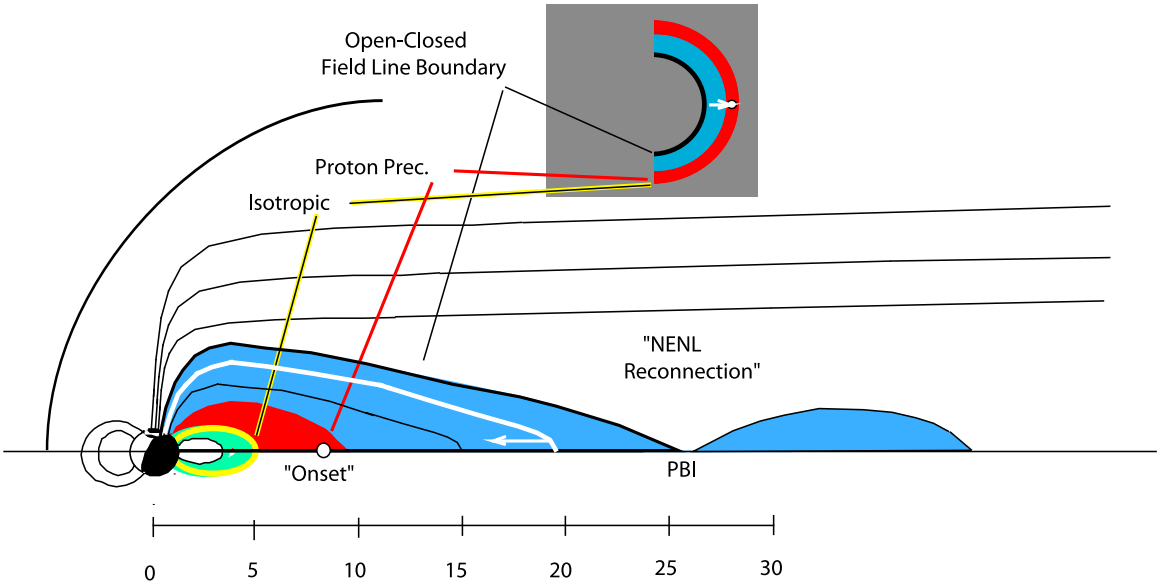

Figure 11. Magnetosphere in which NENL reconnection had occurred and the last closed field line was shortened to about 25–30 R_E. An equatorward propagating feature consistent with the *Nishimura et al.* [2010] paper was added. The substorm "onset" region is illustrated with a red circle and is located in the precipitating proton region.

auroral arc system and substorm intensification instead of AAF onset then we recognize that they are describing the exact same phenomena. *Henderson et al.* [2002] also discuss that at times new "embedded onsets" can be preceded by or perhaps even triggered by flow bursts, but the subsequent expansions of activity is not likely to be a sole consequence of the flows and associated N-S auroral features because all such occurrences do not always result in an auroral onsets. In spite of this prior work, *Nishimura et al.* [2010] contributed by showing that the substorm intensifications prompted by high-latitude precursors are not a rare curiosity but a regularly occurring sequence of events. This is why their statistical results and our reexamination of the validity of their claims are of importance.

[46] We also showed that many of the cases in the *Nishimura et al.* [2010] study were not standalone substorms but the reintensifications of prior substorms. This is relevant because there are several studies in the literature that discuss the properties of N-S arcs and related plasma dynamics that occur during substorm expansion and recovery phases [*Rostoker et al.*, 1987; *Nakamura et al.*, 1993; *Henderson et al.*, 1998]. These studies are relevant because many of the Nisimura events occur in expansion and recovery phase of prior substorms. However, they do not emphasize subsequent reintensifications of the substorm unlike the *Nishimura et al.* [2010] study.

[47] Had all substorms appeared to be triggered by PBI-induced phenomena, we could say that *Nishimura et al.* [2010] are closer to finding the "missing link" between the far down-tail NENL reconnection region (mapping to the polar cap boundary) and the near-tail region (mapping to relatively low latitudes where substorm onsets are observed from the ground). Of course we also find that some substorms seem to occur spontaneously without any of the poleward boundary related precursors. *Elphinstone et al.* [1995b] commented that the PSBL or the open and closed field line boundary may sometimes play an indirect role in substorm onset. This is exactly the case. Furthermore the global scenario described by *Elphinstone et al.* [1995a] seen by the Viking satellite imager including the azimuthally spaced auroral forms (AAFs) could be morphologically identical to the picture described by *Nishimura et al.* [2010] as viewed by high spatial and temporal resolution THEMIS GBO.

[48] In the event that the substorm intensifications are triggered by poleward boundary related precursors, reconnection and NENL formation can shorten the length of last closed field line thus increasing the effectiveness of PBI and plasma flows as triggers. In Figure 10 we schematically illustrate the geometry of the quiescent magnetosphere before substorm onset. During the quiescent phase magnetospheric convection takes place, and reconnection occurs at a distant neutral line at >70 R_e. while the arc where the "onset" would take place is located close to the Earth within the region of proton precipitation at <10 R_E.

[49] In Figure 11 we drew a magnetosphere in which NENL reconnection had occurred and the last closed field line was shortened stretching only to about 25–30 R_E. It should be noted that an observer at the foot of the last closed field line need not necessarily be aware that the field line was shortened. There is a white field line with an inward arrow in Figure 11 showing an equatorward propagating feature consistent with the *Nishimura et al.* [2010] north-south arcs. It is evident that the NENL formation would reduce the propagation distance and propagation time needed to travel from the open and closed field line boundary to the onset region and thus indirectly enhance the probability of triggering.

[50] *Nishimura et al.* [2010] estimate the time delay between PBI and substorm onsets to be 330 s. The propagation velocity in the magnetosphere is given by VFM = $(V^2_A+V^2_s)1/2$, where V_s is the ion acoustic speed = $(kT/m)^{1/2}$ and V_A is the Alfven speed = $B/(4\pi nm)^{1/2}$ [e.g., *Moore et al.*, 1987; *Mende et al.*, 2009]. Both speeds can be calculated by making a few assumptions about the plasma in the magnetotail. For example when P2 encountered the plasma sheet at about 08:45UT on 2 February 2008, it measured a density of about 0.2 cm^{-3} with a strong B_x component of about 20 nT. Therefore, we find that the Alfven speed is relatively low, and the dominant speed is the ion acoustic speed, which is a function of the plasma sheet particle energy. A typical neutral sheet energy is about 5 keV yielding an ion acoustic speed of 600 km/sec. This compares favorably with the results of *Lysak et al.* [2009], who modeled the propagation of Alfven waves in the tail and estimated the fast mode speed to be 650 km/s in the central tail region. Geotail observations suggest that the distant neutral line is about 70–100 R_E downstream on the night side. The time required to propagate from there to the inner magnetosphere is of the order of 700 to 800 s which is too long compared with the observations. If the PBI were at the open-closed field line boundary then the formation of an NENL could contribute by reducing the down tail distance to the source of the trigger.

[51] A possible scenario therefore involves spontaneous reconnection at the NENL (Figure 11). The reconnection at the NENL produces plasma that enters the magnetosphere and needing to travel only 15 Re or less to get to the region where it may or may not trigger a substorm-like intensification. Whether the intensification is triggered or not depends on the status and energy storage of the magnetosphere near the onset region.

[52] The finding that only some of the substorm intensifications are the results of incursion of plasma from the tail suggests that main substorm energization is an independent process and the down tail events are only triggers. The ideas discussed herein therefore make it plausible for substorms to occur deep inside the magnetosphere in the region of closed field lines and at times to respond to external triggers such as reconnection in the near tail [e.g., *Angelopoulos et al.*, 2008]. The central question still remains whether the substorm is an independent instability confined to the inner regions of the magnetsophere that can be triggered by the flows or that the substorm is a direct response of the inner magnetosphere to the flows.

6. Conclusions

[53] Looking at our small sample of cases, we are able to reinterpret some of the findings of *Nishimura et al.* [2010]:

[54] 1. *Nishimura et al.* [2010] highlighted a new feature of substorm development in which a PBI was followed by an equatorward propagation of approximately north-south (N-S) oriented aurora leading to sudden intensification and

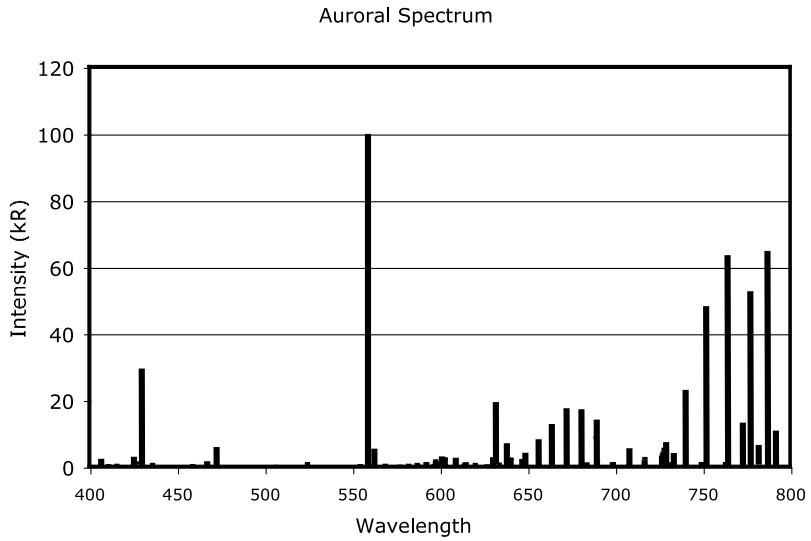

Figure A1. Tabulated spectra from *Vallance Jones* [1973] for a typical IBC III aurora containing 100 kR of 557.7 nm emission.

poleward expansion of a preexisting E-W arc. We verified independently that in a significant number of cases, auroral signatures consistent with this pattern occur. This means that some of these substorm-like intensifications are associated with activity at the poleward auroral boundary, which maps to the instantaneous open-closed field line boundary.

[55] 2. Statistical studies to establish the frequency of these substorm scenarios are handicapped by the limitation of coverage, even with the extensive THEMIS GBO ASI instrumentation. Reinterpreting the *Nishimura et al.* [2010] data, we find that those substorm intensifications which are preceded by N-S oriented auroral forms are less than one half (43%) of all their selected substorm intensifications. When *Nishimura et al.* [2010] included events that do not specifically show N-S features, they obtained a much larger probability of occurrence (84%). When they separated the N-S and E-W events [*Nishimura et al.*, 2010, Figure 7], however, their results were not significantly different from ours.

[56] 3. In our study of 20 randomly selected cases, most that exhibited the above pattern were preceded by substorms with onset time separation of less than 1 h. The intensifications exhibiting the described precursor pattern show typical auroral arc break up and poleward expansion that are characteristics of substorm onset. However, they cannot, therefore, be regarded as isolated substorms.

[57] 4. Space-based imagers, such as the wideband imaging camera on the NASA IMAGE satellite, were not particularly suitable for routine detection of the events described as similar to those by *Nishimura et al.* [2010]. During their normal deployment at full apogee altitude such satellite imagers suffered from lack of spatial resolution and sensitivity. In some special circumstances, however, features with forms that appeared to be consistent with an equatorward moving auroral form intersecting a preexisting E-W arc near the time of substorm onset were detected. During this observation the substorm occurred while the satellite was near perigee at an altitude less than 12,000 km, rapidly moving away from the Earth. Because IMAGE FUV had two minutes cadence, it was impossible to determine the temporal sequence of the precursor event.

[58] In summary, PBIs and subsequent plasma processes appear to be a significant trigger of some substorm intensifications. Although these types of events are frequent contributors to the trigger, a significant number of substorms do not show this trigger pattern and proceed independently from this type of activity.

Appendix A: The Absolute Calibration of the THEMIS GBO ASIs

[59] To estimate whether high-altitude satellite imagers such as the IMAGE FUV experiment would have been able to see these types of phenomena required determination of the absolute intensity of the PBI and associated auroral features. Strictly speaking, accurate calibration of a white light imager in terms of the aurora energy input is impossible because the spectral distribution of the auroral light is variable and in most cases unknown. The variability is due to either the energy of the precipitating electrons or to the composition of the atmosphere. So, different intensity auroras of variable spectral distribution may produce the same response in a particular white light imager. Nevertheless, reasonably accurate estimates can be made because in practice the total energy measured from data taken a by a white light camera, such as the THMEIS GBO ASIs, is surprisingly independent of the auroral spectrum [*Mende et al.*, 2008]. In fact, from model calculations using existing techniques [*Lummerzheim and Lilenstein*, 1994; *Chaston et al.*, 2005], it was found that a typical white light camera response [e.g., *Maggs and Davis*, 1968] varies less than 20% when the auroral mean electron energy is changed from 500 eV to 10 keV. In fact, the largest variations were calculated to be due to changes in atmospheric composition, e.g., mixing ratio of the atomic oxygen. Therefore, considering measurement inaccuracies due to sky transmissions and other extraneous factors we regard electron energy dependence of the combined response for total precipitation

Table A1. The THEMIS GBO Camera Calibration Obtained From the Absolute Calibration Obtained in the Lab Prior to Delivery of the Cameras to the Field Sites[a]

Camera Designator	Counts/kR of 557.7 (nm)	Counts/erg
Cam02	90	54
Cam03	94	57
Cam04	122	73
Cam05	128	77
Cam06	130	78
Cam07	130	78
Cam08	140	84
Cam09	130	78
Cam10	134	81
Cam11	130	78
Cam12	134	80
Cam13	127	77
Cam14	118	71
Cam15	129	78
Cam16	136	82
Cam17	109	65
Cam18	136	82
Cam19	132	80
Cam20	127	77
Cam21	127	76
Cam22	130	78

[a]It was possible to approximately convert a given image into precipitating energy in units of erg cm^{-2} s^{-1}. Note that such conversion is approximate at best.

energy in ergs cm^{-2} s^{-1} as a minor factor. In our study we also neglected the variability of the atmosphere, which is usually caused by large solar storms. We used a "standard aurora" as tabulated by *Vallance Jones* [1973] and shown in Figure A1. These tabulated intensities refer to an IBC III aurora, which contains 100 kR of green line (557.7 nm). Summing up the emissions in the wavelength range of the THEMIS GBOs, from 400 to 800 nm, the equivalent "white light" aurora is 603 kR. Such an aurora contains 30 kR of 427.8 nm emission. Because 180 R of 427.8 nm is approximately equal to 1 erg cm^{-2} s^{-1} [*Rees and Luckey*, 1974], an IBC III aurora of this spectral distribution is equivalent to a precipitating energy of 166 erg cm^{-2} s^{-1}.

[60] To calculate the camera responsivity, we took the Vallance Jones spectra of Figure A1 and multiplied it by the responsivity of each camera. The camera responsivities were obtained with a predeployment calibration procedure in which the camera looked at monochromatic light sources of known intensity. The data are contained in a UCB calibration report titled "THEMIS Ground Based Observatories All-Sky Imager Characterization Report" (thm_gbo_118c_ASI_Char.doc 15 July 2004). The resultant calibration is given in Table A1.

[61] **Acknowledgments.** The authors gratefully acknowledge the outstanding contributions to the THEMIS Ground Based Observatory program from the University of Calgary team under the leadership of E. Donovan. The THEMIS program was supported by NASA under contract NAS5-02099.

[62] Robert Lysak thanks Robert Clauer and another reviewer for their assistance in evaluating this paper.

References

Akasofu, S.-I. (1964), The development of the auroral substorm, *Planet. Space Sci.*, *12*, 273–282, doi:10.1016/0032-0633(64)90151-5.

Akasofu, S. I. (2001), Energy supply processes for solar flares and magnetospheric substorms, *Space Sci. Rev.*, *95*, 613–621, doi:10.1023/A:1005234811265.

Angelopoulos, V., W. Baumjohann, C. F. Kennel, F. V. Coroniti, M. G. Kivelson, R. Pellat, R. J. Walker, H. Lühr, and G. Paschmann (1992), Bursty bulk flows in the inner central plasma sheet, *J. Geophys. Res.*, *97*, 4027–4039, doi:10.1029/91JA02701.

Angelopoulos, V., C. F. Kennel, F. V. Coroniti, R. Pellat, M. G. Kivelson, R. J. Walker, C. T. Russell, W. Baumjohann, W. C. Feldman, and J. T. Gosling (1994), Statistical characteristics of bursty bulk flow events, *J. Geophys. Res.*, *99*, 21,257–21,280, doi:10.1029/94JA01263.

Angelopoulos, V., et al. (2008), Tail reconnection triggering substorm onset, *Science*, *321*, 931–935, doi:10.1126/science.1160495.

Baker, D. N., T. I. Pulkkinen, V. Angelopoulos, W. Baumjohann, and R. L. McPherron (1996), Neutral line model of substorms: Past results and present view, *J. Geophys. Res.*, *101*, 12,975–13,010, doi:10.1029/95JA03753.

Baumjohann, W., G. Paschmann, and C. A. Cattell (1989), Average plasma properties in the central plasma sheet, *J. Geophys. Res.*, *94*, 6597–6606, doi:10.1029/JA094iA06p06597.

Chaston, C. C., et al. (2005), Energy deposition by Alfvén waves into the dayside auroral oval: Cluster and FAST observations, *J. Geophys. Res.*, *110*, A02211, doi:10.1029/2004JA010483.

Donovan, E., et al. (2006), The THEMIS all-sky imaging array-system design and initial results from the prototype imager, *J. Atmos. Sol. Terr. Phys.*, *68*, 1472–1487, doi:10.1016/j.jastp.2005.03.027.

Dungey, J. W. (1961), Interplanetary magnetic field and the auroral zones, *Phys. Rev. Lett.*, *6*, 47–48, doi:10.1103/PhysRevLett.6.47.

Elphinstone, R. D., D. J. Hearn, L. L. Cogger, J. S. Murphree, H. Singer, V. Sergeev, K. Mursula, D. M. Klumpar, G. D. Reeves, and M. Johnson (1995a), Observations in the vicinity of substorm onset: Implications for the substorm process, *J. Geophys. Res.*, *100*, 7937–7969, doi:10.1029/94JA02938.

Elphinstone, R. D., J. S. Murphree, D. J. Hearn, L. L. Cogger, I. Sandahl, P. T. Newell, D. M. Klumpar, S. Ohtani, J. A. Sauvaud, and T. A. Potemra (1995b), The double oval UV auroral distribution: 1. Implications for the mapping of auroral arcs, *J. Geophys. Res.*, *100*, 12,075–12,092, doi:10.1029/95JA00326.

Frey, H. U., S. B. Mende, T. J. Immel, J.-C. Gérard, B. Hubert, S. Habraken, J. Spann, G. R. Gladstone, D. V. Bisikalo, and V. I. Shematovich (2003), Summary of quantitative interpretation of IMAGE far ultraviolet auroral data, *Space Sci. Rev.*, *109*, 255–283, doi:10.1023/B:SPAC.0000007521.39348.a5.

Frey, S., V. Angelopoulos, M. Bester, J. Bonnell, T. Phan, and D. Rummel (2008), Orbit design for the THEMIS mission, *Space Sci. Rev.*, *141*, 61–89, doi:10.1007/s11214-008-9441-1.

Gjerloev, J. W., R. A. Hoffman, J. B. Sigwarth, L. A. Frank, and J. B. H. Baker (2008), A bifurcated oval, *J. Geophys. Res.*, *113*, A03211, doi:10.1029/2007JA012431.

Henderson, M. G., J. S. Murphree, and G. D. Reeves (1994), The activation of the dusk-side and the formation of north-south aligned structures during substorms, in *Proceedings of the Second International Conference on Substorms*, edited by J. R. Kan, J. D. Craven, and S. I. Akasofu, p. 37, Univ. of Alaska Fairbanks, Fairbanks.

Henderson, M. G., G. D. Reeves, and J. S. Murphree (1998), Are north-south aligned auroral structures an ionospheric manifestation of bursty bulk flows?, *Geophys. Res. Lett.*, *25*, 3737–3740, doi:10.1029/98GL02692.

Henderson, M. G., L. Kepko, H. E. Spence, M. Connors, J. B. Sigwarth, L. A. Frank, H. J. Singer, and K. Yumoto (2002), The evolution of north-south aligned auroral forms into auroral torch structures: The generation of omega bands and Ps6 pulsation via flow bursts, in *Proceedings of the Sixth International Conference on Substorms*, edited by R. M. Winglee, pp. 169–174, Univ. of Washington, Seattle.

Hones, E. W., Jr. (1977), Substorm processes in the magnetotail: Comments on 'On hot tenuous plasmas, fireballs, and boundary layers in the Earth's magnetotail' by L. A. Frank, K. L. Ackerson, and R. P. Lepping, *J. Geophys. Res.*, *82*, 5633–5640, doi:10.1029/JA082i035p05633.

Kepko, L., E. Spanswick, V. Angelopoulos, E. Donovan, J. McFadden, K.-H. Glassmeier, J. Raeder, and H. J. Singer (2009), Equatorward moving auroral signatures of a flow burst observed prior to auroral onset, *Geophys. Res. Lett.*, *36*, L24104, doi:10.1029/2009GL041476.

Kornilova, T. A., I. A. Kornilov, and O. I. Kornilov (2006), Auroral intensification structure and dynamics in the double oval: Substorm of December 26, 2000, *Geomagn. Aeron.*, *46*, 450–456, doi:10.1134/S0016793206040062.

Lui, A. T. Y., C.-L. Chang, A. Mankofsky, H.-K. Wong, and D. Winske (1991), A cross-field current instability for substorm expansions, *J. Geophys. Res.*, *96*, 11,389–11,401, doi:10.1029/91JA00892.

Lummerzheim, D., and J. Lilenstein (1994), Electron transport and energy degradation in the ionosphere: Evaluation of the numerical solution, comparison with laboratory experiments and auroral observations, *Ann. Geophys.*, *12*, 1039–1051.

Lysak, R. L., Y. Song, and T. W. Jones (2009), Propagation of Alfvén waves in the magnetotail during substorms, *Ann. Geophys.*, *27*, 2237–2246, doi:10.5194/angeo-27-2237-2009.

Maggs, E., and T. N. Davis (1968), Measurements of the thicknesses of auroral structures, *Planet. Space Sci.*, *16*, 205–206, doi:10.1016/0032-0633(68)90069-X.

McPherron, R. L. (1972), Substorm related changes in the geomagnetic tail: The growth phase, *Planet. Space Sci.*, *20*, 1521–1539, doi:10.1016/0032-0633(72)90054-2.

Mende, S. B., et al. (2000), Far ultraviolet imaging from the IMAGE spacecraft. 2. Wideband FUV imaging, *Space Sci. Rev.*, *91*, 271–285, doi:10.1023/A:1005227915363.

Mende, S. B., et al. (2008), The THEMIS array of ground-based observatories for the study of auroral substorms, *Space Sci. Rev.*, *141*, 357–387.

Mende, S., V. Angelopoulos, H. U. Frey, E. Donovan, B. Jackel, K.-H. Glassmeier, J. P. McFadden, D. Larson, and C. W. Carlson (2009), Timing and location of substorm onsets from THEMIS satellite and ground based observations, *Ann. Geophys.*, *27*, 2813–2830, doi:10.5194/angeo-27-2813-2009.

Moore, T. E., D. L. Gallagher, J. L. Horwitz, and R. H. Comfort (1987), MHD wave breaking in the outer plasmasphere, *Geophys. Res. Lett.*, *14*, 1007–1010, doi:10.1029/GL014i010p01007.

Nagai, T., M. Fujimoto, R. Nakamura, W. Baumjohann, A. Ieda, I. Shinohara, S. Machida, Y. Saito, and T. Mukai (2005), Solar wind control of the radial distance of the magnetic reconnection site in the magnetotail, *J. Geophys. Res.*, *110*, A09208, doi:10.1029/2005JA011207.

Nakamura, R., T. Oguti, T. Yamamoto, and S. Kokubun (1993), Equatorward and poleward expansion of the auroras during auroral substorms, *J. Geophys. Res.*, *98*, 5743–5759, doi:10.1029/92JA02230.

Nishimura, Y., L. Lyons, S. Zou, V. Angelopoulos, and S. Mende (2010), Substorm triggering by new plasma intrusion: THEMIS all-sky imager observations, *J. Geophys. Res.*, *115*, A07222, doi:10.1029/2009JA015166.

Oguti, T. (1973), Hydrogen emission and electron aurora at the onset of the auroral breakup, *J. Geophys. Res.*, *78*, 7543–7547, doi:10.1029/JA078i031p07543.

Pulkkinen, T. I., D. N. Baker, R. J. Pellinen, J. S. Murphree, and L. A. Frank (1995), Mapping of the auroral oval and individual arcs during substorms, *J. Geophys. Res.*, *100*, 21,987–21,994, doi:10.1029/95JA01632.

Rees, M. H., and D. Luckey (1974), Auroral electron energy derived from ratio of spectroscopic emissions: 1. Model computations, *J. Geophys. Res.*, *79*, 5181–5186, doi:10.1029/JA079i034p05181.

Rostoker, G., A. T. Y. Lui, C. D. Anger, and J. S. Murphree (1987), North-south structures in the midnight sector auroras as viewed by the Viking imager, *Geophys. Res. Lett.*, *14*, 407–410, doi:10.1029/GL014i004p00407.

Roux, A., S. Perraut, P. Robert, A. Morane, A. Pedersen, A. Korth, G. Kremser, B. Aparicio, D. Rodgers, and R. Pellinen (1991), Plasma sheet instability related to the westward traveling surge, *J. Geophys. Res.*, *96*, 17,697–17,714, doi:10.1029/91JA01106.

Sergeev, V. A., V. Angelopoulos, J. T. Gosling, C. A. Cattell, and C. T. Russell (1996), Detection of localized, plasma-depleted flux tubes or bubbles in the midtail plasma sheet, *J. Geophys. Res.*, *101*, 10,817–10,826, doi:10.1029/96JA00460.

Shiokawa, K., W. Baumjohann, and G. Haerendel (1997), Braking of high-speed flows in the near-Earth tail, *Geophys. Res. Lett.*, *24*, 1179–1182, doi:10.1029/97GL01062.

Sibeck, D. G., and V. Angelopoulos (2008), THEMIS science objectives and mission phases, *Space Sci. Rev.*, *141*, 35–59, doi:10.1007/s11214-008-9393-5.

Vallance Jones, A. (1973), *Aurora*, pp. 129–140, D. Reidel, Norwell, Mass.

V. Angelopoulos, Institute of Geophysics and Planetary Physics, University of California, Los Angeles, CA 90095, USA.

H. U. Frey and S. B. Mende, Space Sciences Laboratory, University of California, 7 Gauss Way, Berkeley, CA 94720, USA. (mende@ssl.berkeley.edu)

Y. Nishimura, Department of Atmospheric and Oceanic Sciences, University of California, 405 Hilgard Ave., Los Angeles, CA 90095, USA.